

## CHAPTER 6

### RESULTS ON FOURIER TRANSFORM INFRARED SPECTROSCOPY OF POLY( $\epsilon$ -CAPROLACTONE) COMPLEXES

#### 6.1 Introduction

FTIR technique is based on the fact that the molecules of any material absorb energy from infrared radiation that matches the energy of their specific molecular vibration. The outcome of that is the vibration at unique frequencies, which are essentially the fingerprint of designated molecules. Researchers have been utilizing infrared analysis to identify bond types and structures [Julien *et al.*, 1999], examine the interactions among components of a mixture [Deepa *et al.*, 2004] and determine the increase of certain variables from the changes of the area under the band [Chintapalli and Frech, 1996].

In the present work, FTIR spectroscopy has been employed to investigate the interactions between PCL, NH<sub>4</sub>SCN and EC. From thermal studies in chapter 4, new melting peaks have been observed upon addition of NH<sub>4</sub>SCN and EC to PCL-NH<sub>4</sub>SCN and PCL-NH<sub>4</sub>SCN-EC systems respectively. Therefore, PCL is expected to form complexation with NH<sub>4</sub>SCN and EC. The functional carbonyl group, C=O in the structure of PCL has lone pair of electrons in which the oxygen atom is an electronegative atom. It is therefore expected to act as the electron donor and interact with the proton that is bonded covalently with the nitrogen atom of ammonium salt. On the other hand, the ring structure of EC also contains C=O which can allow

complexation with the ammonium salt. All these possible interactions will be studied by observing the changes in position, intensity and shape of the IR spectra.

The intense peak of  $\text{SCN}^-$  stretching mode is used to study the effect of ion association. This peak envelope consists of several possible overlapping bands that represent different ionic species. Thus, curve fitting is applied to separate or deconvolute envelope into individual component bands. The percentage of free ions, ion pairs and ion aggregates are estimated from the area under the respective band. Fig. 6.1 is a representative infrared spectrum that has been curve fitted [Goncalves *et al.*, 2004]. The experimental spectral envelope was first deconvoluted. The fitted spectral envelope could then be reconstructed to check whether the fitting is good. Finally, the individual fitted curve is analyzed according to the respective vibrational modes.

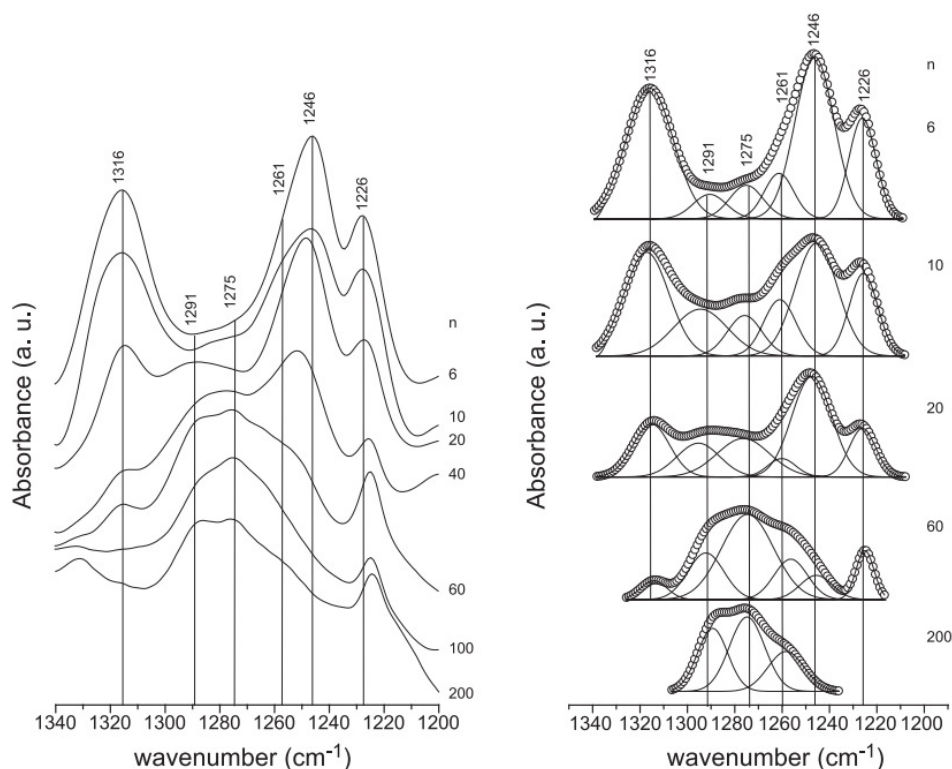


**Fig. 6.1** Room temperature FTIR spectra and curve fitting results of poly(oxyethylene)/siloxane- $\text{Mg}(\text{CF}_3\text{SO}_3)_2$  in the asymmetrical stretching of  $\text{SO}_3$  region.

## 6.2 Infrared studies of pure PCL, NH<sub>4</sub>SCN and THF

In the binary system of PCL-NH<sub>4</sub>SCN, NH<sub>4</sub>SCN is incorporated into PCL during preparation of the polymer electrolytes with THF as solvent. The individual IR spectrum of PCL, NH<sub>4</sub>SCN and THF will be studied prior to the investigation of the PCL-NH<sub>4</sub>SCN systems. Fig. 6.2 and 6.3 presents the infrared spectra of pure PCL membrane without addition of NH<sub>4</sub>SCN salt and the magnified spectrum from 1100 to 1900 cm<sup>-1</sup>, respectively. The chemical structure of PCL is given as inset in Fig. 6.2. The peaks and assignments of the spectra are identified and summarized in Table 6.1.

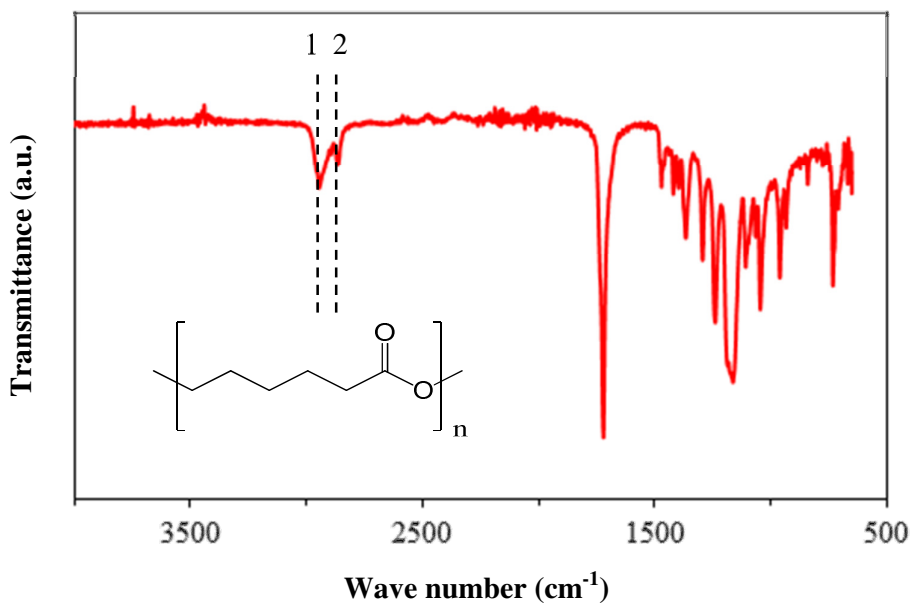


**Fig. 6.2.** Room temperature IR spectra of pure PCL film in the region between 650 and 4000 cm<sup>-1</sup>. Inset presents the chemical structure of PCL.

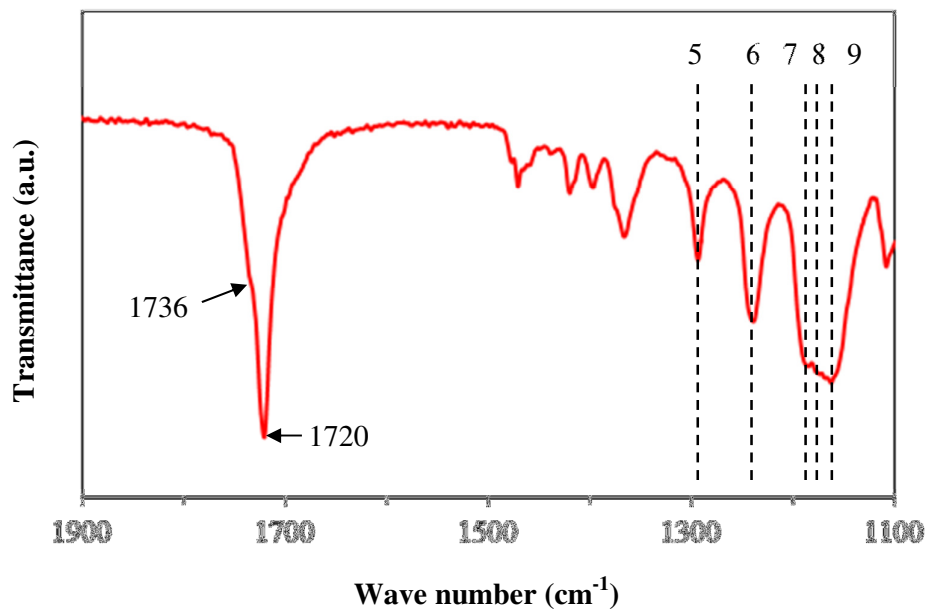


**Fig. 6.3.** Magnified IR spectra of pure PCL film in the region between 1100 and 1900  $\text{cm}^{-1}$ .

**Table 6.1**

Assignments of IR spectra for pure PCL film.

No.	Wave number ( $\text{cm}^{-1}$ )	Assignment	Reference
1	2944	Asymmetric $\text{CH}_2$ stretching	[Wang <i>et al.</i> , 2002]
2	2864	Symmetric $\text{CH}_2$ stretching	[Wang <i>et al.</i> , 2002]
3	1736	Carbonyl, $\text{C}=\text{O}$ stretching, amorphous phase	[Chiu <i>et al.</i> 2004]
4	1720	Carbonyl, $\text{C}=\text{O}$ stretching, crystalline phase	[Chiu <i>et al.</i> 2004])
5	1293	C-O and C-C stretching in the crystalline phase	[Coleman and Zarian, 1979]
6	1239	Asymmetric COC stretching	[Coleman and Zarian, 1979]
7	1190	OC-O stretching	[Coleman and Zarian, 1979]
8	1170	Symmetric COC stretching	[Kuo <i>et al.</i> , 2001]
9	1157	C-O and C-C stretching in the amorphous phase	[Kuo <i>et al.</i> , 2001]

From Fig. 6.2, the strongest band is given by C=O stretching mode. From the magnified IR spectrum as shown in Fig. 6.3, the carbonyl stretching has two phases, the amorphous phase depicted as a small shoulder at  $1736\text{ cm}^{-1}$  and the crystalline phase depicted as a sharp intense peak at  $1720\text{ cm}^{-1}$ . This is in agreement with the report by Chiu *et al.* (2004).

According to Chiu, the pure PCL demonstrates two carbonyl stretching bands at  $1734\text{ cm}^{-1}$  (also as a small shoulder) and  $1724\text{ cm}^{-1}$ . These two bands correspond to the amorphous and crystalline conformations, respectively. The interaction of polymer-salt is expected to occur at this carbonyl function group of PCL.

The backbone of C-O-C polyester group is observed at various locations in the IR spectrum in the region between  $1150$  and  $1300\text{ cm}^{-1}$ . According to Elzein and co-workers (2004), the location of the C-O-C polyester group can only be observed if the region between  $1150$  and  $1200\text{ cm}^{-1}$  is deconvoluted. These C-O-C groups can also be a possible complexation site for the cation of the salt.

The FTIR spectrum of  $\text{NH}_4\text{SCN}$  and THF are presented in Fig. 6.4 with inset showing the chemical structure of  $\text{NH}_4\text{SCN}$  and THF. The assignment of vibrational modes are given in Table 6.2.

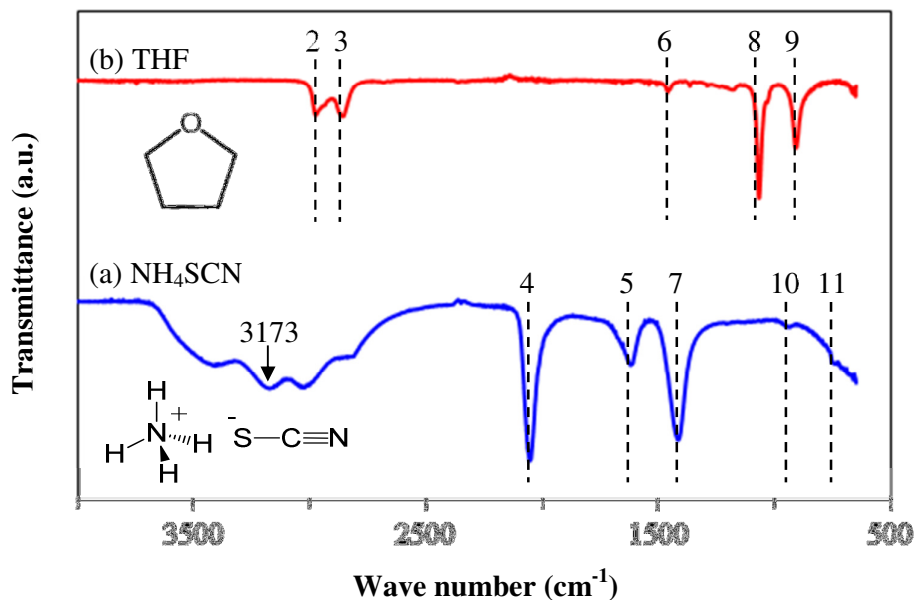


**Fig. 6.4.** Room temperature IR spectra of (a)  $\text{NH}_4\text{SCN}$  and (b) THF in the region between 650 and 4000  $\text{cm}^{-1}$ . Insets present the respective chemical structures.

**Table 6.2**

Assignments of IR spectra for  $\text{NH}_4\text{SCN}$  and THF.

No.	Wave number ( $\text{cm}^{-1}$ )		Assignment	Reference
	THF	$\text{NH}_4\text{SCN}$		
1	-	3173	NH stretching	[Awadhia and Agrawal, 2007]
2	2958	-	Asymmetric $\text{CH}_2$ stretching	[Shurvell and Southby, 1997]
3	2865	-	Symmetric $\text{CH}_2$ stretching	[Shurvell and Southby, 1997]
4	-	2052	Asymmetric $\text{C}\equiv\text{N}$ stretching	[Zhang and Wang, 2009]
5	-	1619	Asymmetric $\text{C}\equiv\text{N}$ stretching	[Zhang and Wang, 2009]
6	1446	-	$\text{CH}_2$ deformation	[Shurvell and Southby, 1997]
7	-	1415	NH deformation	[Zhang and Wang, 2009]
8	1065	-	Ring stretching	[Shurvell and Southby, 1997]
9	905	-	Ring breathing	[Shurvell and Southby, 1997]
10	-	948	Symmetric SCN bending	[Awadhia and Agrawal, 2007]
11	-	752	C-S stretching	[Awadhia and Agrawal, 2007]

The two dominant strong peaks at  $905\text{ cm}^{-1}$  and  $1065\text{ cm}^{-1}$  indicate the ring structures of THF as reported by Shurvell and Southby (1997). In the study of PCL- $\text{NH}_4\text{SCN}$  complexes, these strong ring stretching and ring breathing peaks will be used as an indicator to trace the existence of THF in the complexes.

For ammonium salt, it can be seen that the N-H stretching at  $3173\text{ cm}^{-1}$  overlaps with the O-H stretching mode of water which shows a broad peak between  $2500$  and  $3700\text{ cm}^{-1}$  [Lappi *et al.*, 2004]. This reviews the hygroscopic nature of the salt. The strong and intense peak at  $2052\text{ cm}^{-1}$  will be deconvoluted to study different ionic species in PCL- $\text{NH}_4\text{SCN}$  complexes.

### 6.3 Infrared studies of PCL- $\text{NH}_4\text{SCN}$ system

Fig. 6.5 and 6.6 depict the infrared spectra in the region from  $700$  to  $1500\text{ cm}^{-1}$  and  $1570$  to  $3400\text{ cm}^{-1}$ , respectively, of the pure  $\text{NH}_4\text{SCN}$  and PCL- $\text{NH}_4\text{SCN}$  complexes with various salt concentrations, recorded at room temperature.

From Fig. 6.5, the strong N-H deformation peak at  $1415\text{ cm}^{-1}$  of the pure salt is found to overlap with PCL spectrum in all the compositions. The relative intensity of the polymer complexes in the region between  $1350$  and  $1450\text{ cm}^{-1}$  increases with addition of salt content up to 32 wt.%. This observation could be attributed to the ion-dipole interaction between  $\text{NH}_4^+$  and the polar group of PCL.

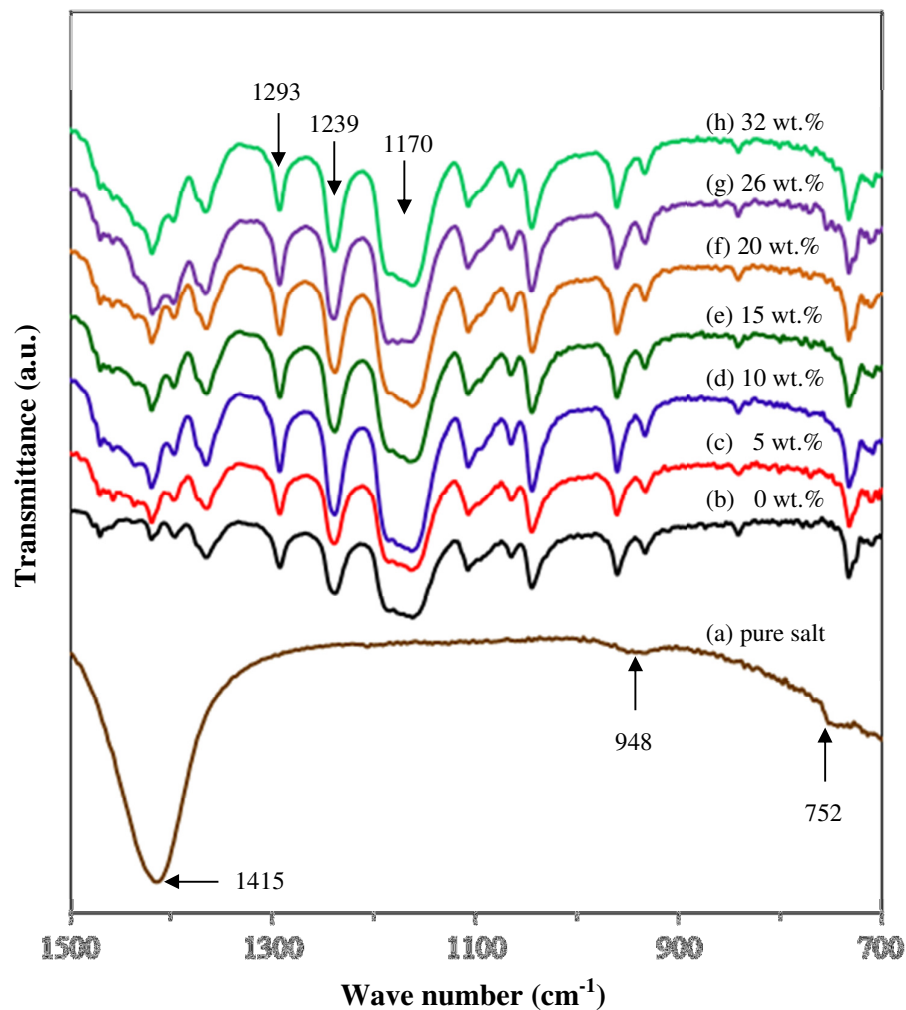


**Fig. 6.5.** Evolution of room temperature IR spectra of (a)  $\text{NH}_4\text{SCN}$  and PCL- $\text{NH}_4\text{SCN}$  films added with 0 to 32 wt.%  $\text{NH}_4\text{SCN}$  in the region between 700 and 1500  $\text{cm}^{-1}$ .

No obvious changes of the IR spectra in the region from 1150 to 1300  $\text{cm}^{-1}$  of the C-O-C group. The two weak peaks at 948  $\text{cm}^{-1}$  and 752  $\text{cm}^{-1}$  of the ammonium salt become unnoticeable in the polymer-salt system. This suggests the salt has solvated into the polymer matrix. The two strong ring stretching and ring breathing peaks of THF at 905  $\text{cm}^{-1}$  and 1065  $\text{cm}^{-1}$  are not observed in the entire salt concentration. This indicates the solvent compound does not exist in the complexes.

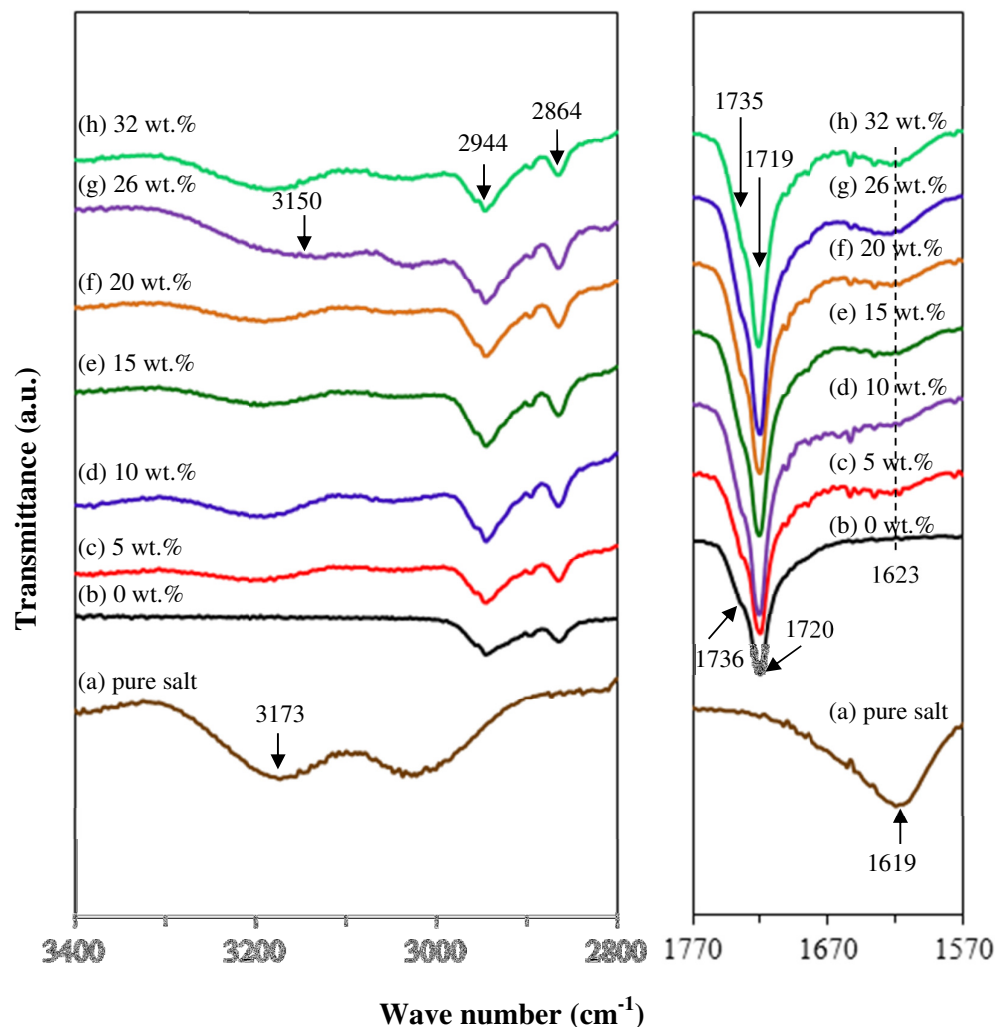


**Fig. 6.6.** Evolution of room temperature IR spectra of (a)  $\text{NH}_4\text{SCN}$  and PCL- $\text{NH}_4\text{SCN}$  films added with 0 to 32 wt.%  $\text{NH}_4\text{SCN}$  displaying N-H stretching and carbonyl stretching regions.

Referring to Fig. 6.6, the N-H stretching region (from 2800 to 3400  $\text{cm}^{-1}$ ) at 3173  $\text{cm}^{-1}$  has downshifted to lower wavenumber 3150  $\text{cm}^{-1}$  upon addition of 26 wt.% salt. The spectral region from 1570 to 1770  $\text{cm}^{-1}$  of PCL includes the carbonyl stretching mode. Upon addition of  $\text{NH}_4\text{SCN}$  to PCL, both carbonyl bands (crystalline and amorphous conformations) maintain at 1736 and 1720  $\text{cm}^{-1}$  with a gradual increase

in relative intensity. At the same time, a new shoulder peak appears at  $1623\text{ cm}^{-1}$  and become more visible at higher salt content.

The new shoulder peak could be attributed to the loosely-bound coordinate bond (or dative covalent bond) between C=O of PCL and  $\text{NH}_4^+$  through one of the H atom. This reflects the interaction between the polymer and salt. The carbonyl group of PCL acts as bond acceptor and the H atom of the  $\text{NH}_4^+$  cation acts as bond donor. This complexation grows with the addition of  $\text{NH}_4\text{SCN}$ . Such phenomenon is observed in many literatures.

In PCL- $\text{LiClO}_4$  system, Chiu *et al.* (2004) did not observe any obvious spectral shifts of the carbonyl bands at  $1724\text{ cm}^{-1}$  and  $1734\text{ cm}^{-1}$ . Instead, a new shoulder appeared at  $1700\text{ cm}^{-1}$  upon addition of  $\text{LiClO}_4$  to PCL-based polymer electrolytes. The intensity of this shoulder was observed to increase with increasing  $\text{Li}^+$  salt. The researchers then concluded that the appearance of new shoulder was due to the interaction between the  $\text{Li}^+$  and C=O of PCL.

IR analysis of Wu and Chang (2007) and Lin and Wu (2011) showed an emergence of new shoulder at  $1705\text{ cm}^{-1}$  on all their four polyester- $\text{LiClO}_4$  binary systems. The four types of polyester were poly (ethylene adipate) (PEA), poly (1,4-butylene adipate) (PBA), poly (1,6-hexamethylene adipate) (PHA) and PCL. This shoulder became more visible as more  $\text{Li}^+$  salt was added. According to these researchers, the free carbonyl band was observed to maintain at  $1730\text{ cm}^{-1}$  and the new shoulder at  $1705\text{ cm}^{-1}$  was attributed to “ $\text{Li}^+$  bonded” carbonyl band. Thus the interaction between polyester and  $\text{Li}^+$  salt was proven.

For the present system, the appearance of new shoulder at  $1623\text{ cm}^{-1}$  implies that complexation occurs between PCL and  $\text{NH}_4\text{SCN}$ . This conclusion is in good agreement with DSC results in section 4.2 (Fig. 4.2).

From the above analysis, the cation of the salt is believed to interact with the oxygen atom in  $\text{C}=\text{O}$  of PCL via coordinate bond as proposed in Fig. 6.7. This ion-dipole interaction can be easily dissociated upon an applied electric field. Thus, cation can jump from one PCL- $\text{NH}_4\text{SCN}$  complex site to surrounding free site, leaving a vacant site to be filled by another cation from nearby site. Eventually, it diffuses through the polymer matrix forming a flow of charge.

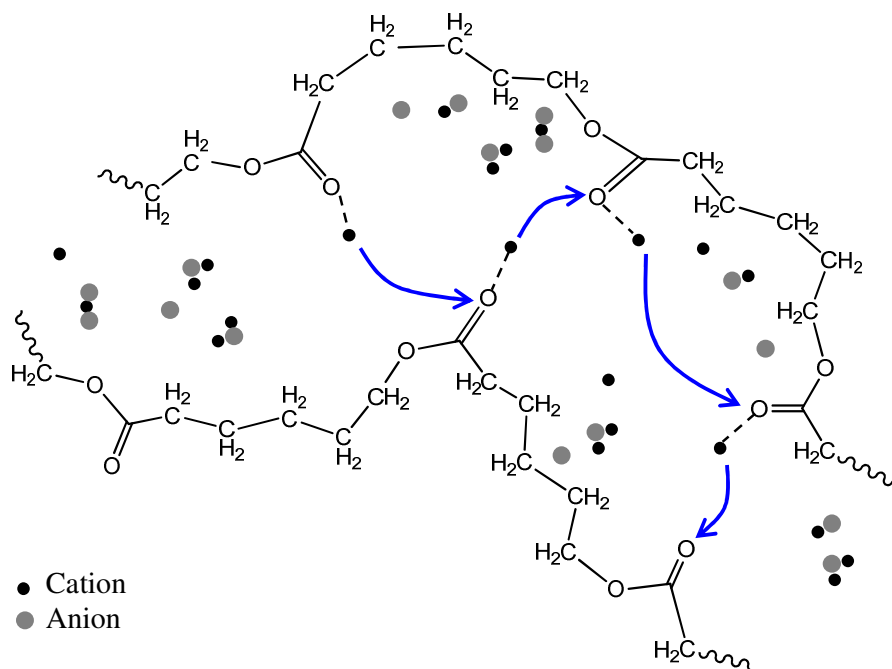


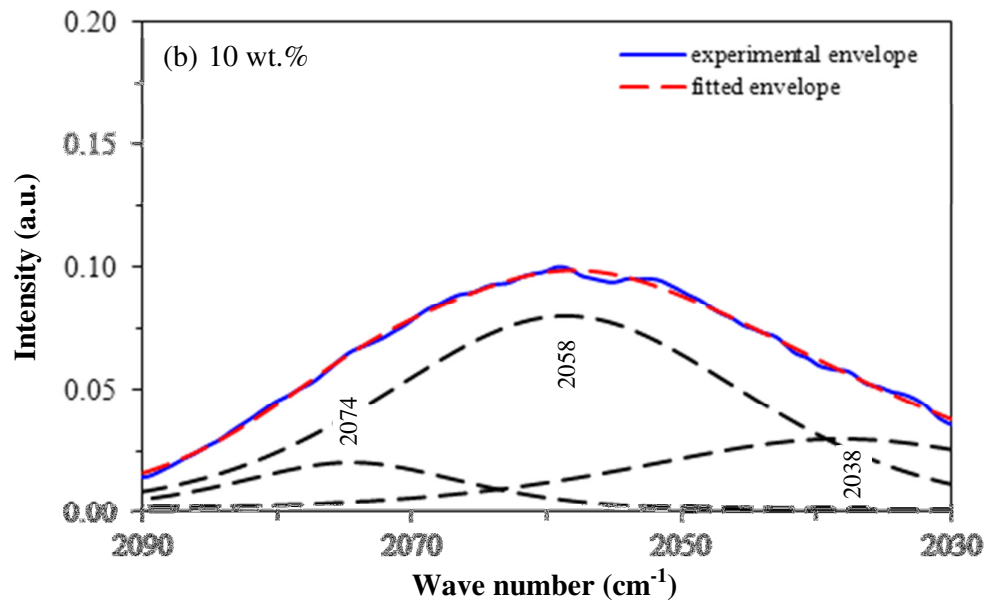
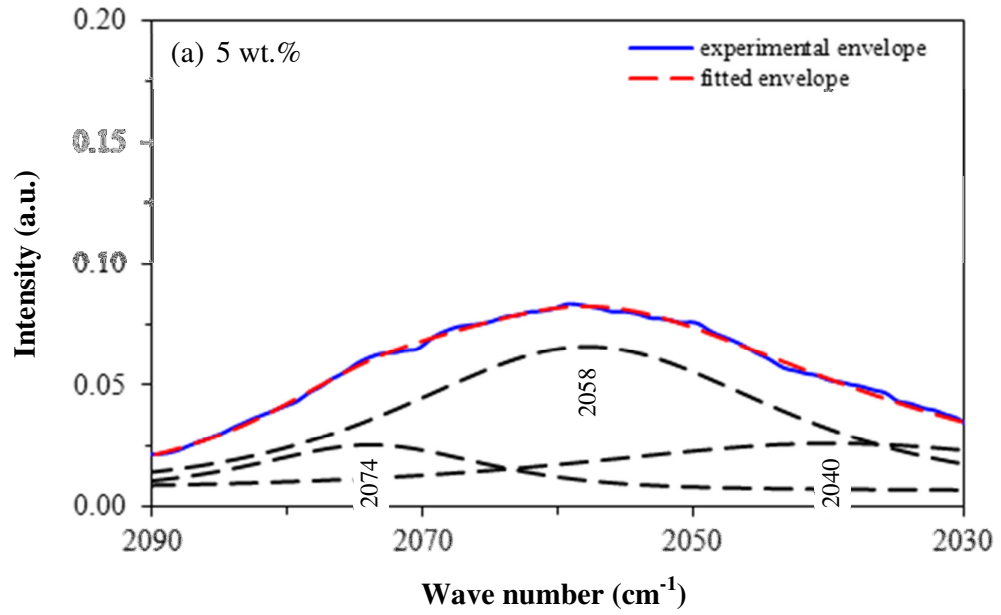
**Fig. 6.7.** Schematic representation of the cation coordination in PCL- $\text{NH}_4\text{SCN}$  polymer complex. The dotted line represents the ion-dipole interaction between cation and PCL. Arrow shows the direction of the cation movement.

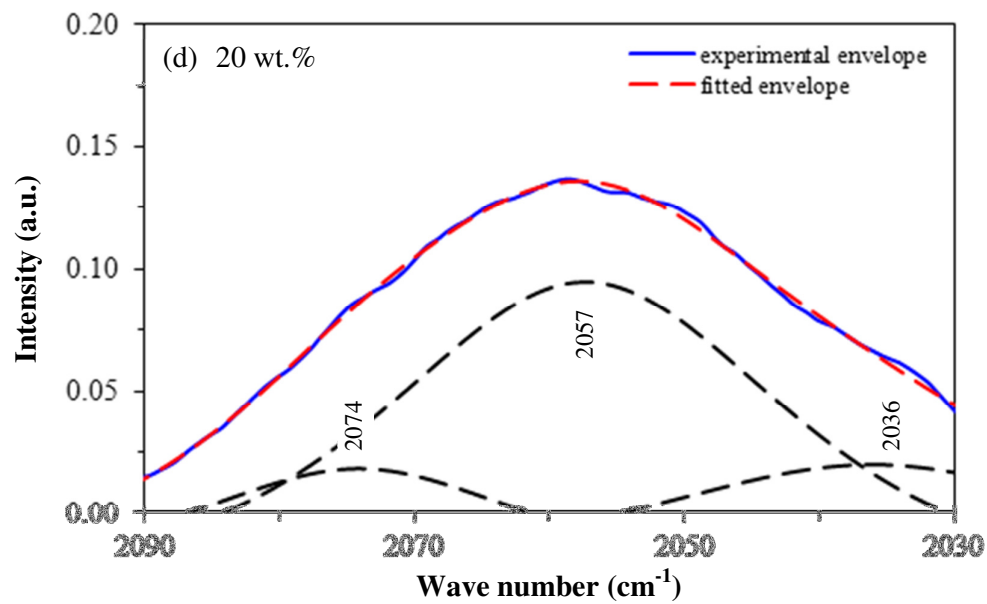
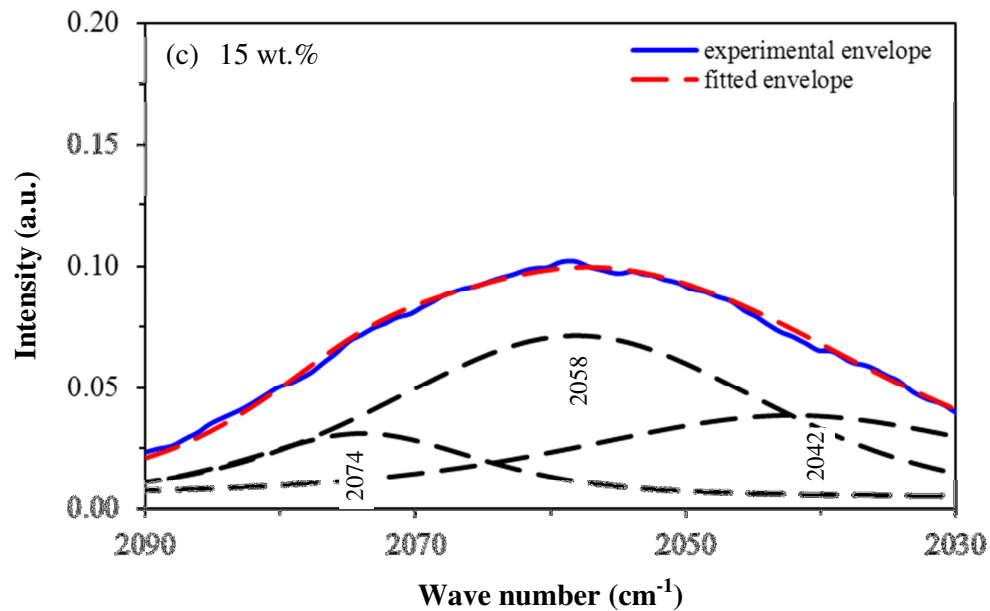
SCN<sup>-</sup> is called an ambident linear anion because it contains two alternative reactive sites. It can form many complexes such as S-bonding (CS stretching), N-bonding (CN stretching) and bridge complexes of the S and N atom (SCN bending). It is therefore a good candidate to study the effect of ion dissociation in PE system [Ramya *et al.*, 2007].

The IR spectra of the present system show a broad peak at the SCN<sup>-</sup> stretching mode region, from 2030 to 2090 cm<sup>-1</sup>. According to the literature [Cruickshank *et al.*, 1995; Xu *et al.*, 1996; Zhang *et al.*, 2003; Ramya *et al.*, 2007], this broad envelope is a result of overlapping of three narrower peaks. These peaks are located at ~2040 cm<sup>-1</sup>, ~2058 cm<sup>-1</sup> and ~2074 cm<sup>-1</sup> representing the free anions (SCN<sup>-</sup>), contact ion pairs (NH<sub>4</sub><sup>+</sup> SCN<sup>-</sup>) and ion aggregates, respectively. Thus, a process of deconvolution is carried out to separate the convoluted peaks.

Firstly, the overlapping transmittance spectra in the SCN<sup>-</sup> stretching mode region is converted into absorbance spectra. The baseline is then corrected for all respective IR spectrum. Finally, the OMNIC software is used to carry out the separation by selecting constant base line and Gaussian-Lorentzian peak type.

Fig. 6.8 shows the curve-fitted IR spectra of SCN<sup>-</sup> stretching modes in PCL-NH<sub>4</sub>SCN films added with 0 to 32 wt.% salt. The experimental data is described by the solid line while dotted lines represent the curve-fitting data.





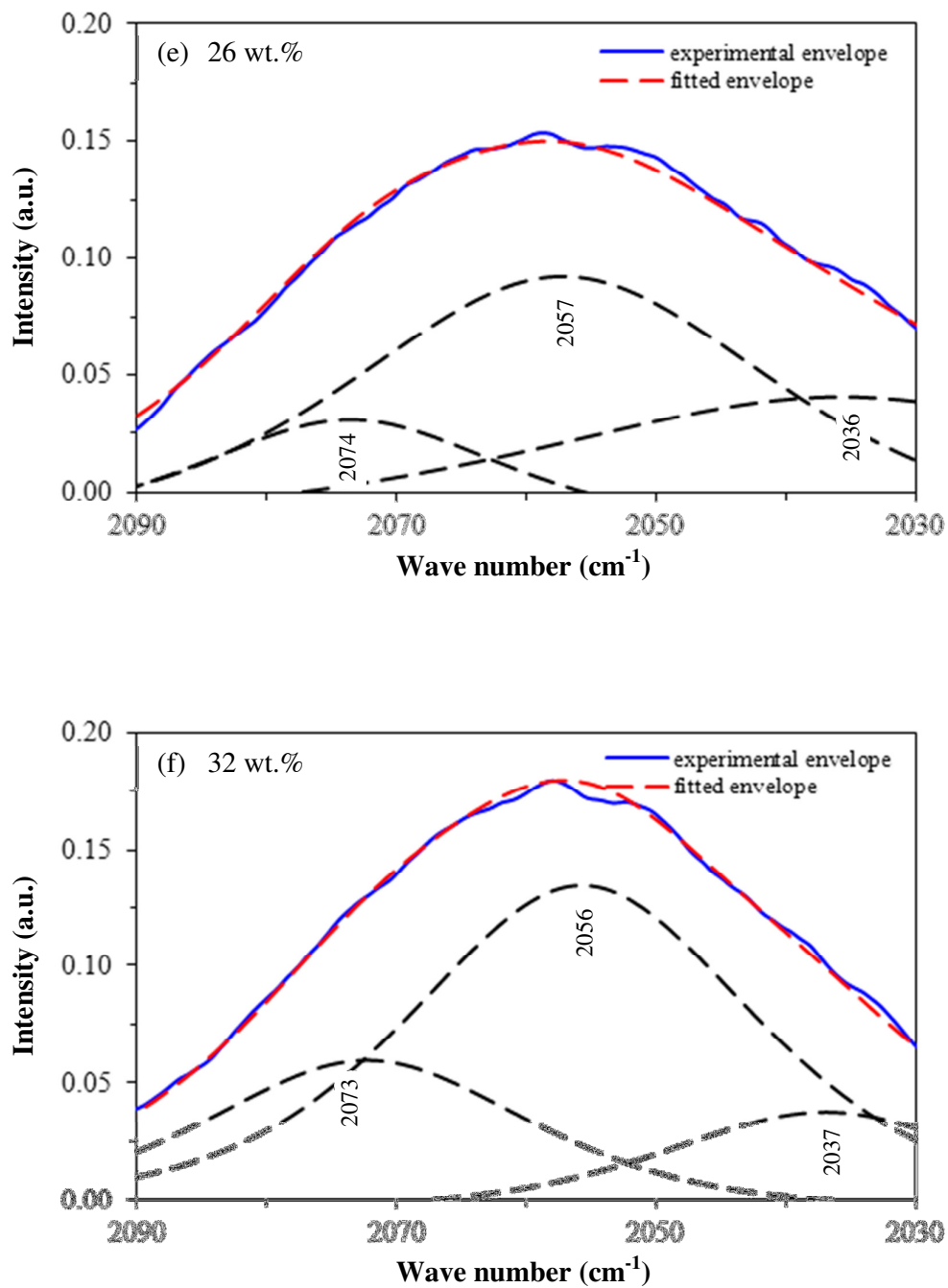


**Fig. 6.8.** The curve-fitting IR spectra of PCL-NH<sub>4</sub>SCN films added with 0 to 32 wt.% NH<sub>4</sub>SCN displaying CN stretching modes.

The percentage of ionic species is calculated by taking the fraction of the integral area under the curve. This percentage is believed to be proportional to the relative concentration of ionic species. The results of individual fitted curve are displayed in Fig. 6.9 as a function of salt concentration.

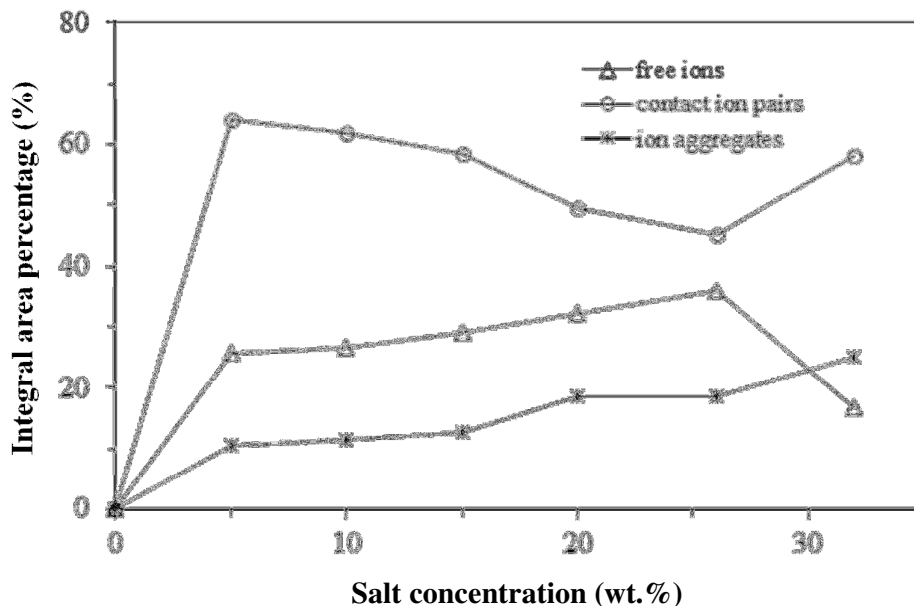


**Fig. 6.9.** Integral area percentage of free ions, contact ion pairs and ion aggregates as a function of salt concentration for PCL-NH<sub>4</sub>SCN system.

At 5 wt.% salt, free ions, contact ion pairs and ion aggregates record a percentage of 25.6, 63.9 and 10.5 %, respectively. As more salt is added, the integral percentage area of free ions rises consistently to 26.6, 28.9, 32.0 and 36.0 % at 10, 15, 20, 26 wt.% salt, respectively. On the other hand, the number of contact ion pairs decreases gradually to 61.9, 58.4, 49.5 and 45.3 % at 10, 15, 20 and 26 wt.% salt, respectively. The integral area percentage of ion aggregates is found to keep increasing to 11.5, 12.7, 18.5 and 18.7 % at 10, 15, 20 and 26 wt.% salt. This means the percentage

of free ions and ion aggregates increase with increasing salt content at the expense of contact ion pairs. The correlation between different ionic species seems clear. When the percentage of the charged free ions become maximum at 26 wt.% salt, the neutral contact ion pairs records a minimum.

At 32 wt.% salt, the percentage of free ions shows a drastic turn, dropping from 36.0 to 16.7 %. At the same time, both percentage of ion pairs and ion aggregates increase to 58.2 and 25.1 %. Similar results were reported by Ramya *et al.* (2007) in PVP-NH<sub>4</sub>SCN system and Chen-Yang *et al.* (2009) in PAN-LiClO<sub>4</sub>-ALA-MMT system. The present deconvolution results suggest that addition of salt up to a critical value (26 wt.%) injects more corresponding free ions into polymer matrix. Beyond that, the free ions are too close to one another, forming ion pairs and higher aggregates through the attraction of coulombic force. Thus, when the number of free ions displays a drop after 26 wt.% salt, both number of contact ion pairs and ion aggregates increase. This percentage of different ionic species could give an insight in conductivity studies in Chapter 7.

#### 6.4 Infrared studies of EC

The IR spectrum of pure EC is shown in Fig. 6.10 and the assignments of vibrational modes are tabulated in Table 6.3. According to Huang *et al.* (1996), the carbonyl stretching mode of EC is split into two peaks at 1783 cm<sup>-1</sup> and 1764 cm<sup>-1</sup> due to Fermi resonance caused by dipole-dipole coupling of EC molecules. Various CH<sub>2</sub> modes are observed in the region from 1550 cm<sup>-1</sup> to 1200 cm<sup>-1</sup>. There are two ring

stretching modes and two ring breathing modes revealing the cyclic ring structure of EC.

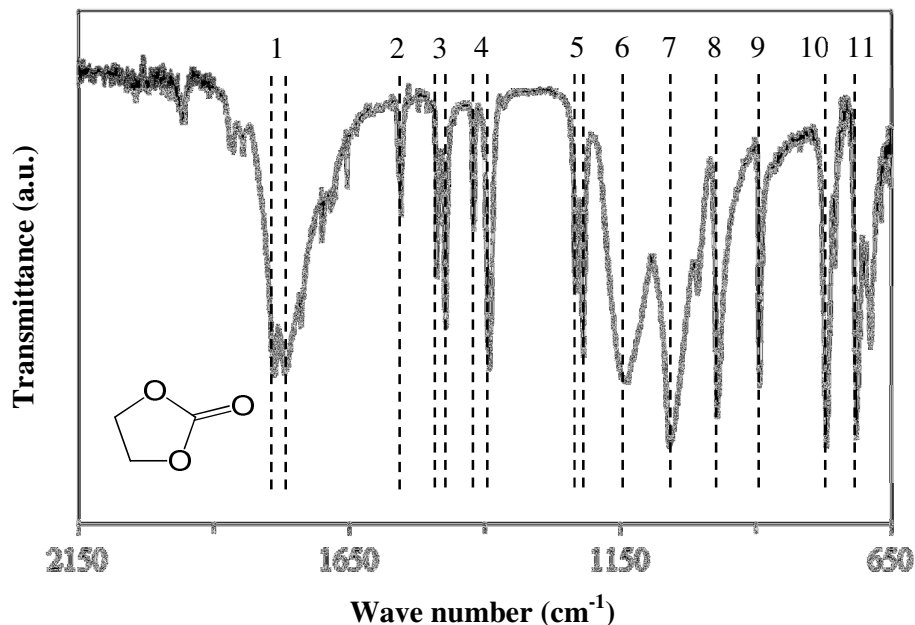


**Fig. 6.10.** Room temperature IR spectra of pure EC in the region between 650 and 2150 cm<sup>-1</sup>. Inset presents the chemical structure of EC.

**Table 6.3**

Assignments of FTIR spectra for pure EC.

No.	Wave number (cm <sup>-1</sup> )	Assignment	Reference
1	1784, 1766	Carbonyl, C=O stretching	[Huang <i>et al.</i> 1996]
2	1552	CH <sub>2</sub> scissoring	[Masia <i>et al.</i> , 2004]
3	1486, 1470	CH <sub>2</sub> bending	[Angell, 1956]
4	1419, 1389	CH <sub>2</sub> wagging	[Wang <i>et al.</i> , 1996]
5	1230, 1216	CH <sub>2</sub> twisting	[Masia <i>et al.</i> , 2004]
6	1139	Ring stretching	[Masia <i>et al.</i> , 2004]
7	1054	Ring breathing	[Wang <i>et al.</i> , 1996]
8	968	Skeletal stretching	[Huang <i>et al.</i> 1996]
9	892	Ring breathing	[Wang <i>et al.</i> , 1996]
10	767	Ring stretching	[Idris <i>et al.</i> , 2007]
11	712	C=O bending	[Huang <i>et al.</i> 1996]

### 6.5 Infrared Studies of PCL-EC system

Interaction between PCL and EC are investigated by adding 10 wt.% and 30 wt.% of EC to the PCL films. Fig. 6.11 shows the FTIR spectra recorded at room temperature for pure EC, pure PCL and PCL films added with 10 wt.% and 30 wt.% EC.

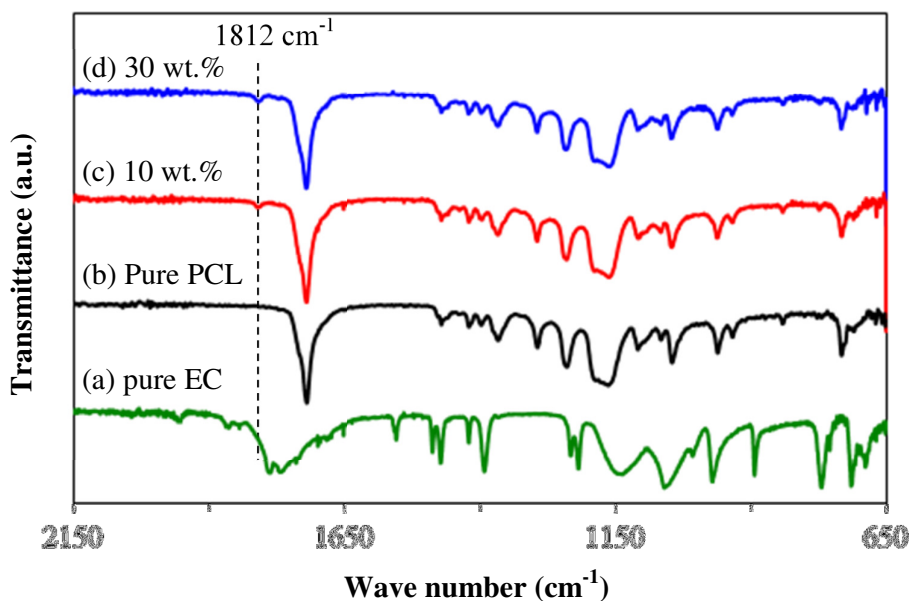


**Fig. 6.11.** Room temperature IR spectra of (a) pure EC, (b) pure PCL and PCL-EC films added with (c) 10 wt.% and (d) 30 wt.% EC in the region between 650 and 2150  $\text{cm}^{-1}$ .

Several researchers found that no interaction occurs between the polymer host and plasticizer in polymer electrolyte systems such as grafted natural rubber, MG30 and EC [Kumutha and Alias, 2006]. They observed little or no difference in the IR spectra of the polymer electrolytes upon addition of EC. However, some literature reported that interactions between polymer and plasticizer do occur. As an example, Wang *et al.* (1999) experimentally found that polymer-plasticizer interactions occurred between the cyano ( $\text{C}\equiv\text{N}$ ) group of PAN with the carbonyl ( $\text{C}=\text{O}$ ) group of EC, PC and DMF.

In the present system as shown in Fig. 6.11, PCL films added with 10 wt.% and 30 wt.% EC demonstrates minimum or no difference in the IR spectra region from 650 to 1750  $\text{cm}^{-1}$ . A new peak appears at 1812  $\text{cm}^{-1}$  upon addition of 10 wt.% EC to PCL film. The intensity of this peak increases with increasing EC content as presented in Fig. 6.12. This new peak could be contributed from the C=O stretching of EC that is upshifted from 1784  $\text{cm}^{-1}$ , showing an interaction between the PCL and EC, making the EC ring stiffer [Wang *et al.* 1999].

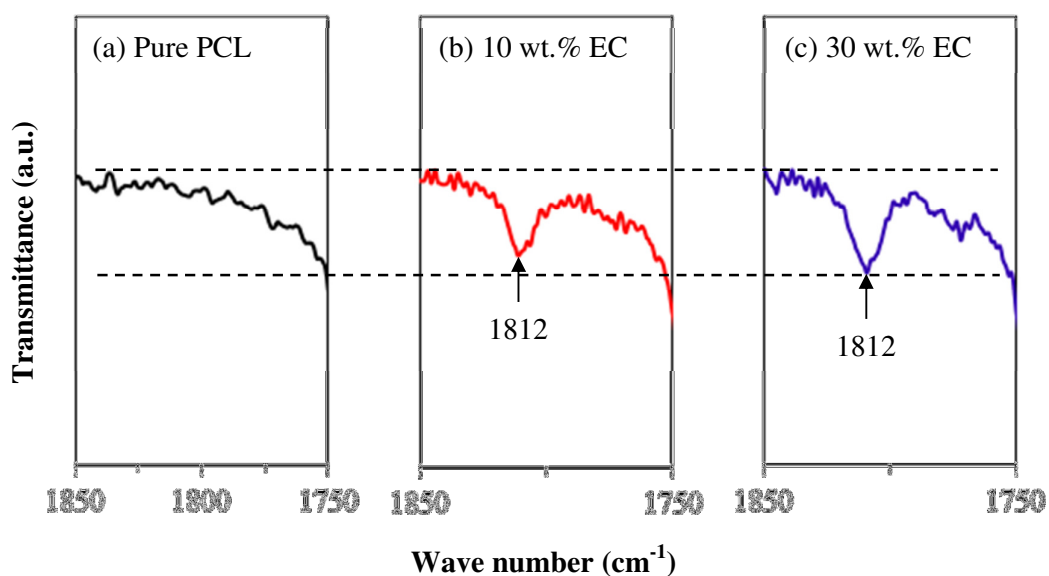


**Fig. 6.12.** Magnified IR spectra of (a) pure PCL, PCL-EC films added with (b) 10 wt.% and (c) 30 wt.% EC in the region between 1750 and 1850  $\text{cm}^{-1}$ .

## 6.6 Infrared Studies of EC-NH<sub>4</sub>SCN system

The interactions between EC and NH<sub>4</sub>SCN are examined by adding 10 wt.% and 30 wt.% ammonium salt to EC that was heated to 40 °C. Fig. 6.13 exhibits the room

temperature FTIR spectra of pure EC and EC added with 10 wt.% and 30 wt.%  $\text{NH}_4\text{SCN}$ .

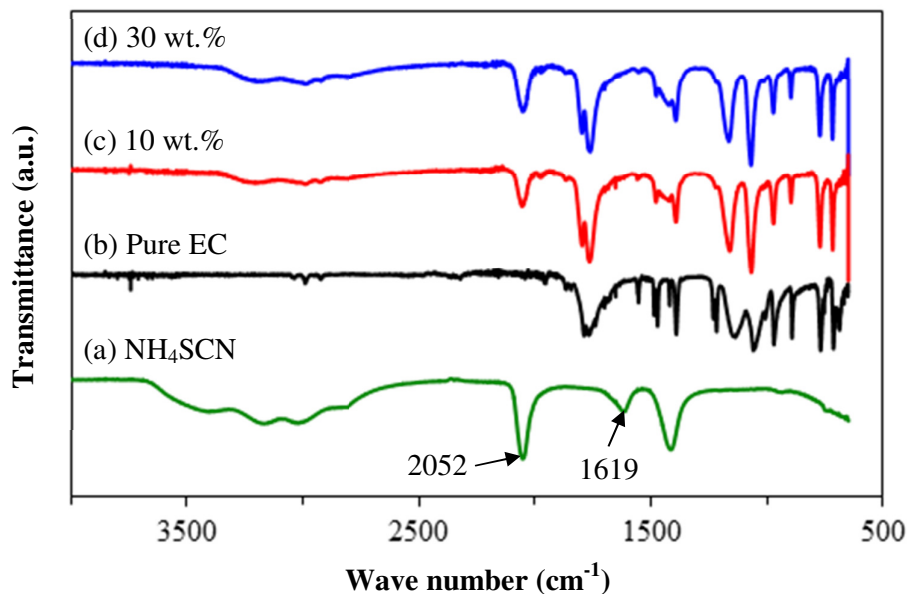


**Fig. 6.13.** Room temperature IR spectra of (a)  $\text{NH}_4\text{SCN}$ , (b) pure EC and EC- $\text{NH}_4\text{SCN}$  electrolyte added with (c) 10 wt.% and (d) 30 wt.%  $\text{NH}_4\text{SCN}$ .

Fig. 6.13 shows large wavenumber shifts in the IR spectra, indicating interactions between the ammonium salt and EC. Upon incorporation of 10 wt.%  $\text{NH}_4\text{SCN}$  to EC, a clear peak at  $2052\text{ cm}^{-1}$  appears due to the asymmetric  $\text{C}\equiv\text{N}$  stretching of the salt. The intensity of this peak increases with increasing salt content as expected. However, this cyano stretching mode at  $1619\text{ cm}^{-1}$  is observed to diminish in EC electrolyte. In order to observe the wavenumber changes clearly, the magnified IR spectra in the region between  $1600\text{ to }2000\text{ cm}^{-1}$ ,  $1200\text{ to }1600\text{ cm}^{-1}$  and  $1190\text{ to }690\text{ cm}^{-1}$  are depicted in Fig. 6.14, 6.15 and 6.16 respectively. The IR spectra with corresponding wavenumber changes for EC added with 10 wt.% and 30 wt.%  $\text{NH}_4\text{SCN}$  is listed in Table 6.4.

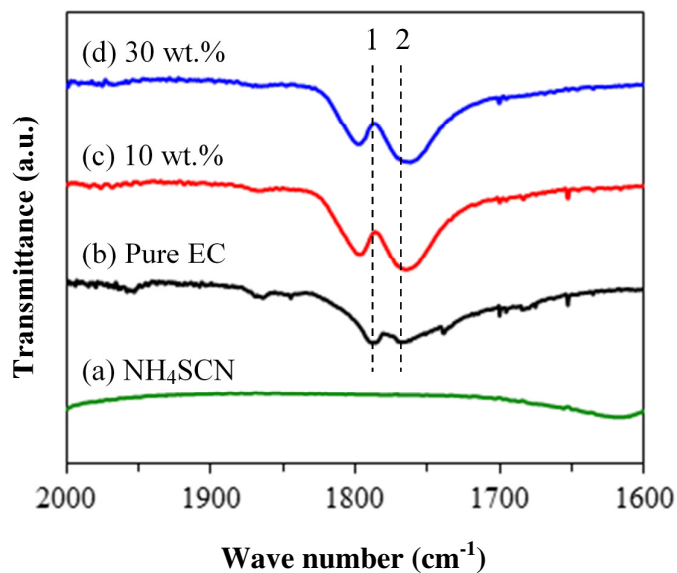


**Fig. 6.14.** Magnified IR spectra of (a) NH<sub>4</sub>SCN, (b) pure EC and EC-NH<sub>4</sub>SCN electrolyte added with (c) 10 wt.% and (d) 30 wt.% NH<sub>4</sub>SCN in the region between 1600 and 1800 cm<sup>-1</sup>.

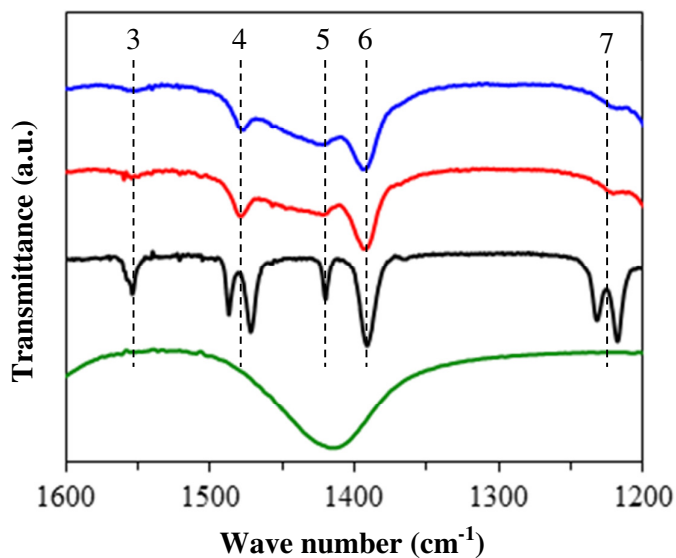


**Fig. 6.15.** Magnified IR spectra of (a) NH<sub>4</sub>SCN, (b) pure EC and EC-NH<sub>4</sub>SCN electrolyte added with (c) 10 wt.% and (d) 30 wt.% NH<sub>4</sub>SCN in the region between 1200 and 1600 cm<sup>-1</sup>.

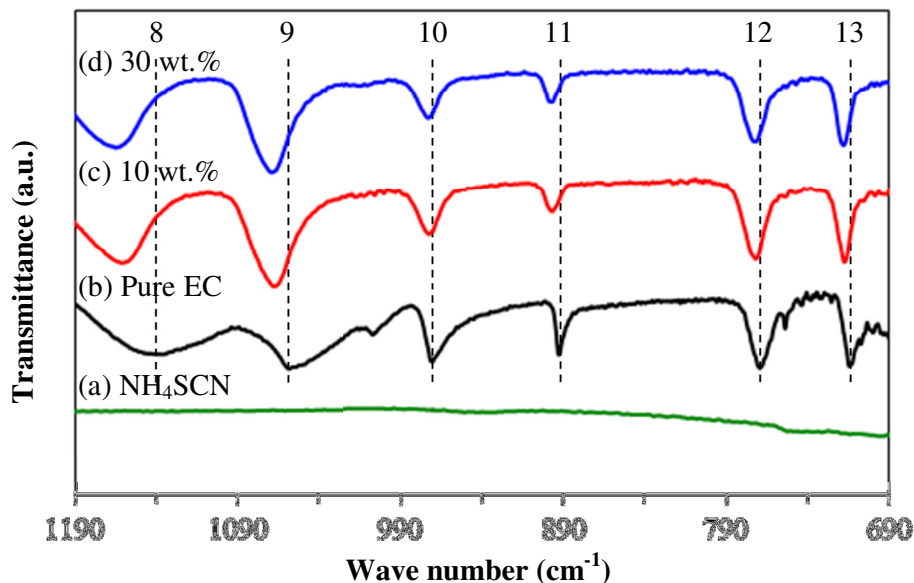


**Fig. 6.16.** Magnified IR spectra of (a)  $\text{NH}_4\text{SCN}$ , (b) pure EC and EC- $\text{NH}_4\text{SCN}$  electrolyte added with (c) 10 wt.% and (d) 30 wt.%  $\text{NH}_4\text{SCN}$  in the region between 690 and 1190  $\text{cm}^{-1}$ .

**Table 6.4**

IR spectra with corresponding wavenumber changes for EC- $\text{NH}_4\text{SCN}$  electrolyte added with 10 wt.% and 30 wt.%  $\text{NH}_4\text{SCN}$ .

No.	Assignments	Wave number ( $\text{cm}^{-1}$ )			Remarks
		Pure EC	10 wt.% $\text{NH}_4\text{SCN}$	30 wt.% $\text{NH}_4\text{SCN}$	
1	C=O stretching	1784	1795	1795	Upshift 11 $\text{cm}^{-1}$
2	C=O stretching	1766	1763	1760	Downshift 6 $\text{cm}^{-1}$
3	$\text{CH}_2$ scissoring	1552	1552	1552	Peak intensity reduces
4	$\text{CH}_2$ bending	1486, 1470	1476	1474	2 peaks merge to single peak
5	$\text{CH}_2$ wagging	1419	1419	1419	Peak intensity reduces
6	$\text{CH}_2$ wagging	1389	1389	1389	Peak become broaden
7	$\text{CH}_2$ twisting	1230, 1216	1218	1218	2 peaks merge to a shoulder
8	Ring stretching	1139	1158	1161	Upshift 22 $\text{cm}^{-1}$
9	Ring breathing	1054	1066	1067	Upshift 13 $\text{cm}^{-1}$
10	Skeletal stretching	968	971	971	Upshift 3 $\text{cm}^{-1}$
11	Ring breathing	892	897	897	Upshift 5 $\text{cm}^{-1}$
12	Ring stretching	767	770	771	Upshift 4 $\text{cm}^{-1}$
13	C=O bending	712	716	717	Upshift 5 $\text{cm}^{-1}$

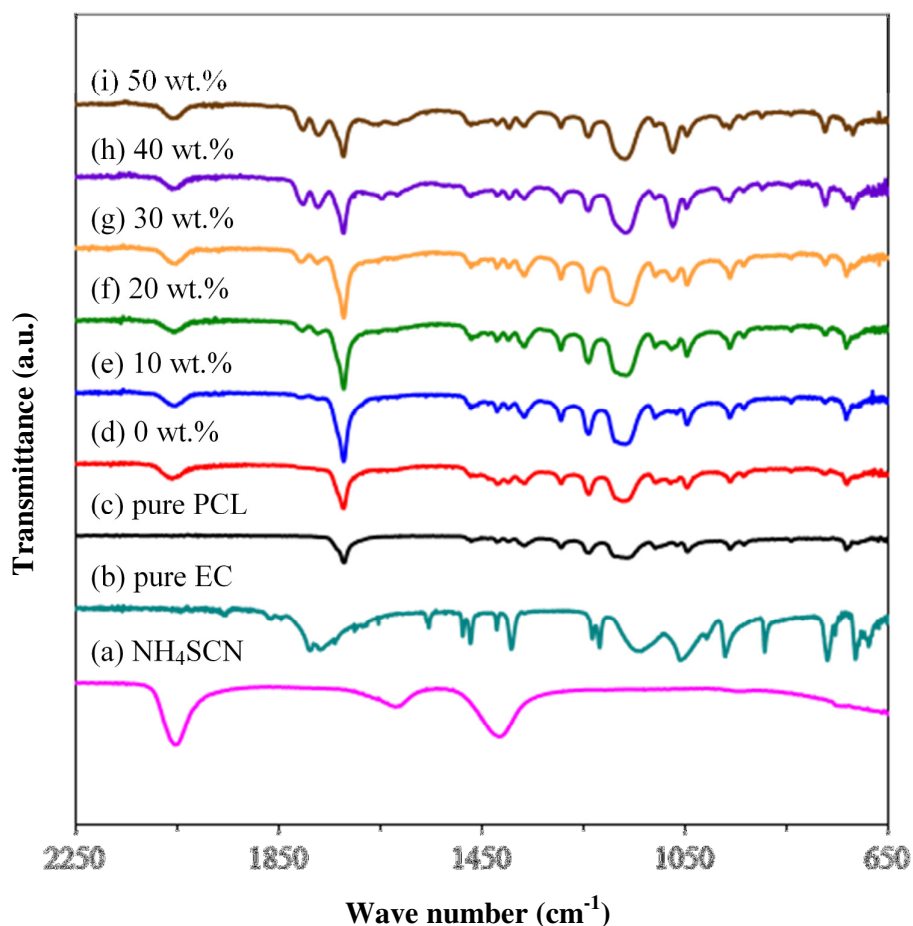
As can be seen in Fig.6.14, the one of two C=O stretching of EC at  $1784\text{ cm}^{-1}$  upshifts to  $1795\text{ cm}^{-1}$  ( $+\Delta 11\text{ cm}^{-1}$ ) but the other EC carbonyl band at  $1766\text{ cm}^{-1}$  is downshifted to  $1760\text{ cm}^{-1}$ . The relative intensity of both carbonyl bands increase with increasing EC content.

CH<sub>2</sub> modes of EC in Fig. 6.15 exhibit various responses with addition of NH<sub>4</sub>SCN. The CH<sub>2</sub> scissoring at  $1552\text{ cm}^{-1}$  remains at the same wavenumber, but with reduction in intensity while the two CH<sub>2</sub> bending modes originally located at  $1486\text{ cm}^{-1}$  and  $1470\text{ cm}^{-1}$  merge to a single peak at  $1474\text{ cm}^{-1}$ . No significant changes of the CH<sub>2</sub> wagging at  $1419\text{ cm}^{-1}$  and  $1389\text{ cm}^{-1}$  are observed. CH<sub>2</sub> twisting bands at  $1230\text{ cm}^{-1}$  and  $1216\text{ cm}^{-1}$  merge into a shoulder at  $1218\text{ cm}^{-1}$ .

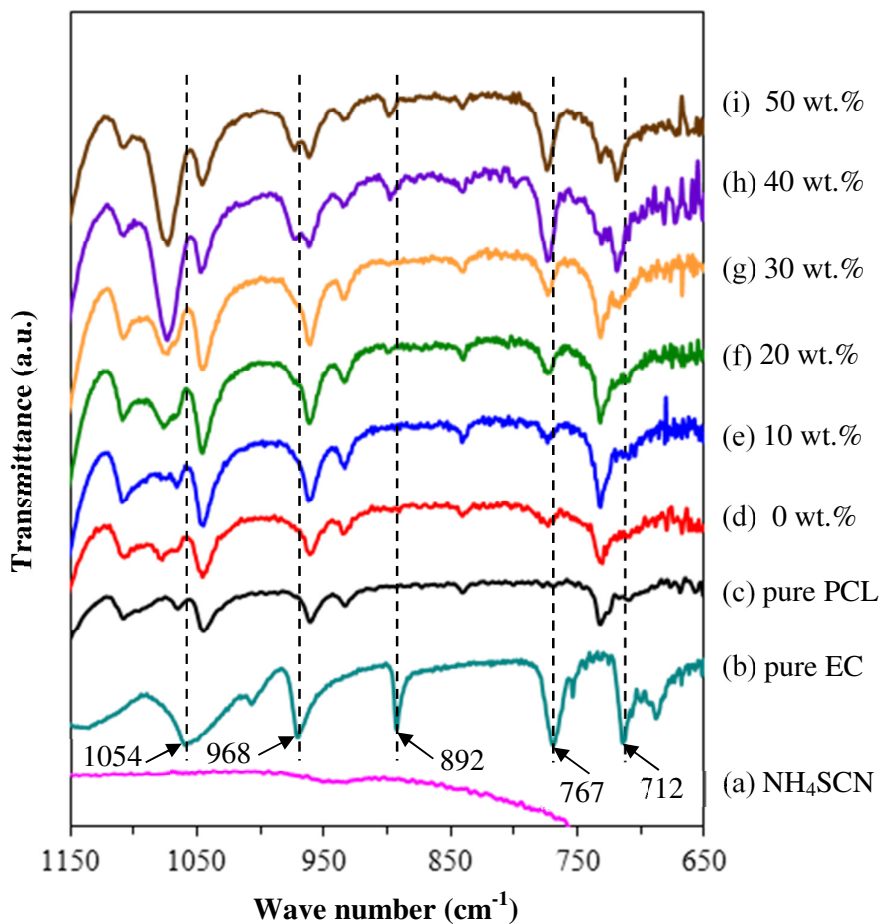
It is interesting to note that in Fig. 6.16, the ring stretching of EC at  $1139\text{ cm}^{-1}$  shows a large position upshift to  $1161\text{ cm}^{-1}$  ( $+\Delta 22\text{ cm}^{-1}$ ) while the same stretching mode at  $767\text{ cm}^{-1}$  upshift slightly to  $771\text{ cm}^{-1}$ . Both ring breathing bands at  $1054\text{ cm}^{-1}$  and  $892\text{ cm}^{-1}$  shift to higher wavenumber at  $1067\text{ cm}^{-1}$  and  $897\text{ cm}^{-1}$ , respectively. Skeletal stretching mode is observed to upshift marginally from  $968\text{ cm}^{-1}$  to  $971\text{ cm}^{-1}$  and finally the bending mode of carbonyl move slightly from  $712\text{ cm}^{-1}$  to  $717\text{ cm}^{-1}$ . All the ring stretching, ring breathing and skeletal stretching modes from  $690$  to  $1190\text{ cm}^{-1}$  shift to higher wavenumber. This seems to show that the interaction between EC and salt making the ring structure of EC stiffer, thus requiring more energy for vibration.

### 6.7 Infrared Studies of PCL-NH<sub>4</sub>SCN-EC system

Fig 6.17 shows the IR spectra of PCL-NH<sub>4</sub>SCN-EC polymer electrolytes in the region between 650 and 2250 cm<sup>-1</sup> whereby the interaction between PCL, NH<sub>4</sub>SCN and EC will be investigated. These PE films contain fixed amount of PCL and NH<sub>4</sub>SCN, 1.00 g and 0.35 g respectively, but different concentrations of EC varying from 0 to 50 wt.%. The magnified IR spectra in the region from 650 to 1150 cm<sup>-1</sup> are depicted in Fig. 6.18.



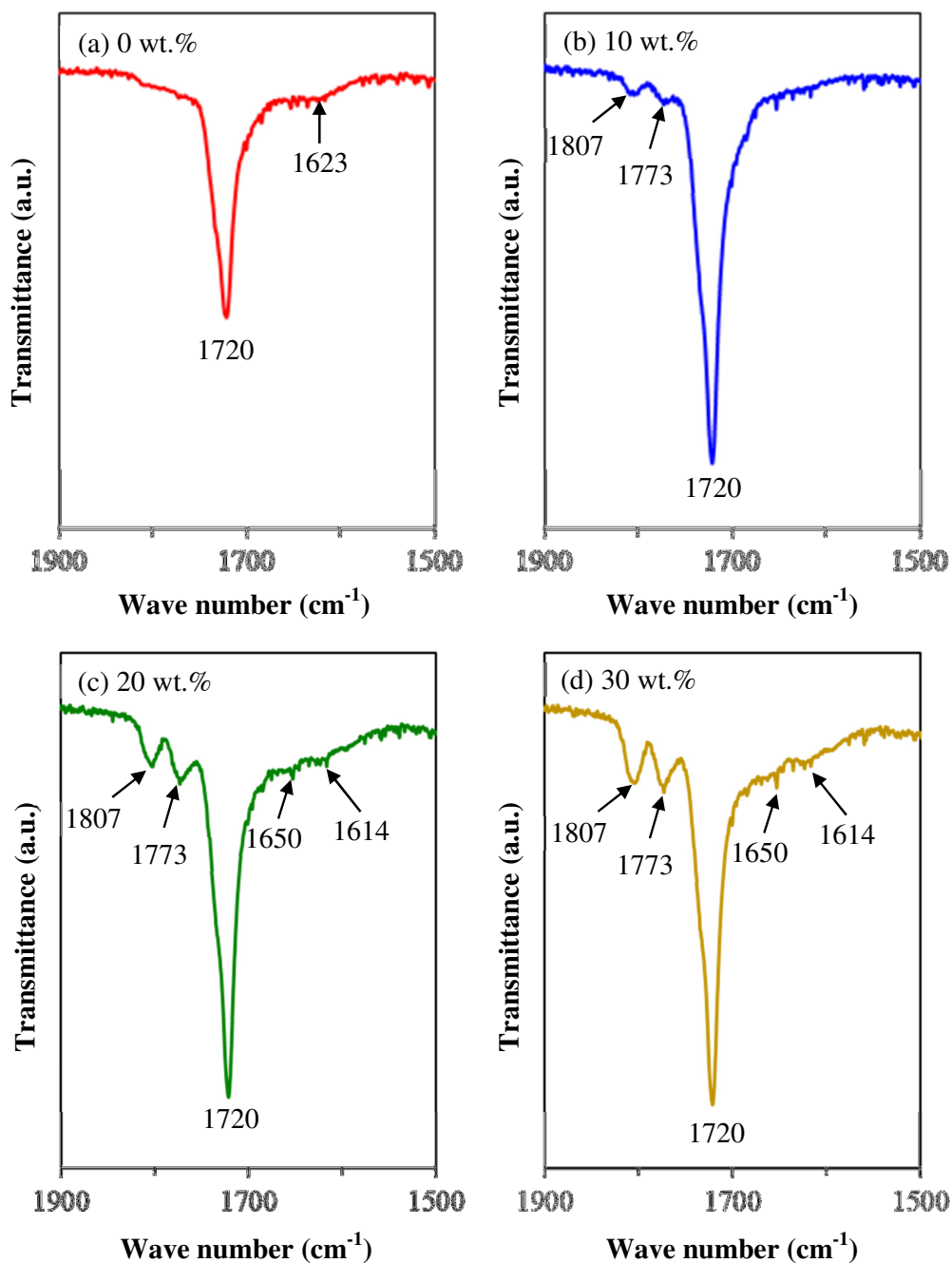
**Fig. 6.17.** Evolution of room temperature IR spectra of (a) NH<sub>4</sub>SCN, (b) pure EC, (c) pure PCL and PCL-NH<sub>4</sub>SCN-EC films added with 0 to 50 wt.% EC.



**Fig. 6.18.** Magnified IR spectra of PCL-NH<sub>4</sub>SCN-EC films added with 0 to 50 wt.% EC in the region between 650 and 1150 cm<sup>-1</sup>.

All of the spectral changes within this region are similar to the interactions between EC and NH<sub>4</sub>SCN, as elucidated in the earlier section. The ring breathing bands upshift from 1054 cm<sup>-1</sup> and 892 cm<sup>-1</sup> to 1068 cm<sup>-1</sup> and 896 cm<sup>-1</sup>, respectively, skeletal stretching mode upshifts from 968 cm<sup>-1</sup> to 971 cm<sup>-1</sup>, ring stretching mode upshifts from 767 cm<sup>-1</sup> to 771 cm<sup>-1</sup> and carbonyl bending mode upshifts from 712 cm<sup>-1</sup> to 717 cm<sup>-1</sup>. As such, PCL does not seem to alter the interaction between EC and NH<sub>4</sub>SCN within this region.

The interactions between PCL,  $\text{NH}_4\text{SCN}$  and EC in the region between 1500 and  $1900\text{ cm}^{-1}$  would be interesting because both PCL and EC contain carbonyl bond that may compete to interact with the  $\text{NH}_4^+$  via coordinate bond. Fig. 6.19 shows the IR spectra of PCL-  $\text{NH}_4\text{SCN}$ -EC systems added with 0 to 50 wt.% EC in the region from 1500 to  $1900\text{ cm}^{-1}$ .



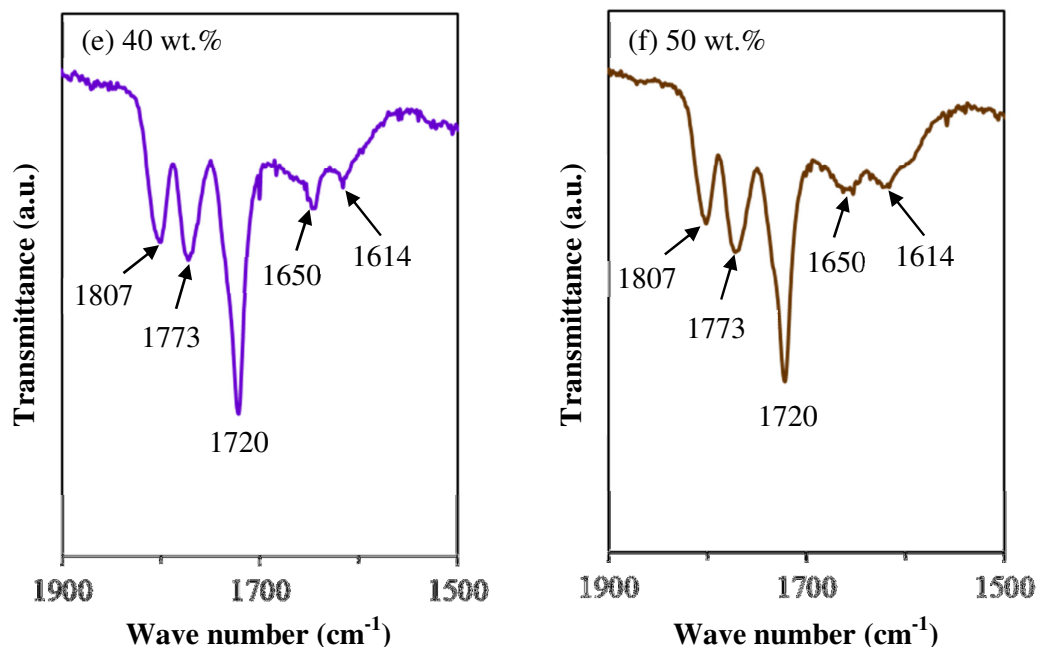


**Fig. 6.19.** Magnified IR spectra of PCL-NH<sub>4</sub>SCN-EC films added with 0 to 50 wt.% EC in the region between 1500 and 1900 cm<sup>-1</sup>.

Upon addition of 10 wt.% EC to the PCL-NH<sub>4</sub>SCN system, the C=O stretching band of PCL at 1720 cm<sup>-1</sup> remain unshifted but shows a rise in intensity. On the other hand, the peak at 1623 cm<sup>-1</sup> is observed to be very weak. To recall back from Fig. 6.6, evidence of interaction between C=O of PCL and NH<sub>4</sub><sup>+</sup> upon addition of NH<sub>4</sub>SCN has been manifested through the new peak appearance at 1623 cm<sup>-1</sup>. This suggests that EC has weakened the interaction between PCL and NH<sub>4</sub>SCN.

In addition, two new peaks appear at 1773 cm<sup>-1</sup> and 1807 cm<sup>-1</sup>. The 1773 cm<sup>-1</sup> new peak could be attributed to the upshift of C=O stretching band of EC from 1766 cm<sup>-1</sup> as a result of interaction between EC and NH<sub>4</sub>SCN of the PCL-NH<sub>4</sub>SCN system. It is interesting to note that the original 1766 cm<sup>-1</sup> peak of EC is observed to move to lower wavenumber to 1760 cm<sup>-1</sup> in the studies of EC-NH<sub>4</sub>SCN system in the earlier section. The second new peak at 1807 cm<sup>-1</sup> could be due to the interaction between PCL

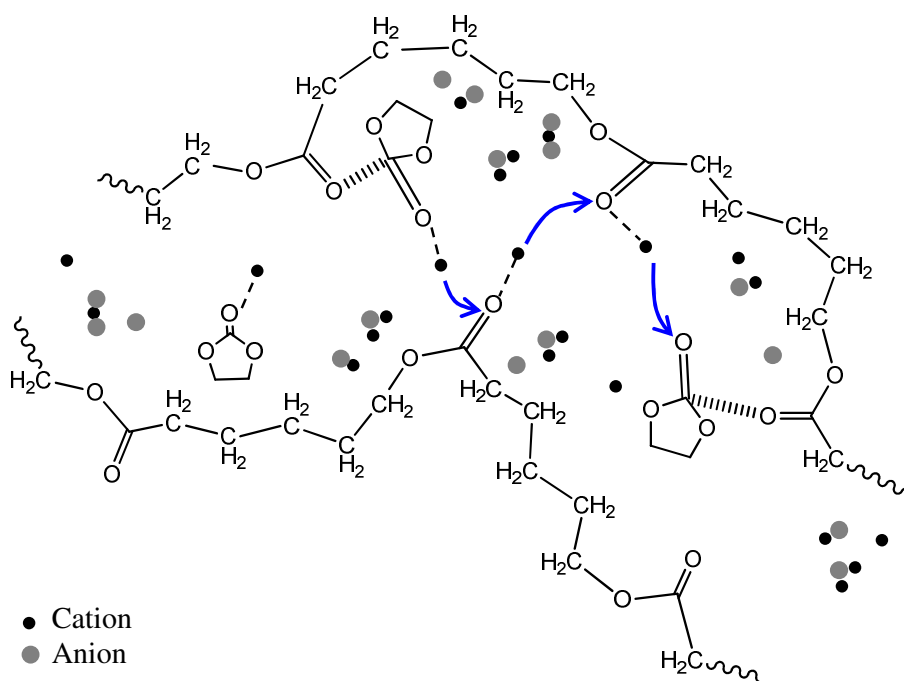
and EC, an upshift of the C=O stretching of EC from  $1784\text{ cm}^{-1}$ . This interaction is also supported by DSC studies earlier in section 4.3 (Fig.4.6) in which the appearance of multiple  $T_m$  is attributed to the new PCL-EC complex phases.

The weakening of PCL-NH<sub>4</sub>SCN interaction at  $1623\text{ cm}^{-1}$  and the strengthening of EC-NH<sub>4</sub>SCN interaction at  $1773\text{ cm}^{-1}$  seems to show that EC is a stronger competitor than PCL for interaction with NH<sub>4</sub><sup>+</sup> of the ammonium salt. This shows that the addition of EC leads to the formation of EC-NH<sub>4</sub><sup>+</sup> complex which will reduce the fraction of PCL-NH<sub>4</sub><sup>+</sup> complex. Therefore, the flexibility of PCL chains increases as shown in Fig. 4.5 with lower  $T_g$  value. Similar observation was made by Qian *et al.* (2002) in PEO-LiClO<sub>4</sub>-EC system. A decrease of PEO-Li<sup>+</sup> complex was reported due to the formation of Li<sup>+</sup>-EC complex and lead to the lowering  $T_g$ .

When 20 and 30 wt.% EC is incorporated, the carbonyl stretching band of PCL remain unshifted at  $1720\text{ cm}^{-1}$ , strong in intensity and a pair of doublet peaks at  $1614\text{ cm}^{-1}$  and  $1650\text{ cm}^{-1}$  start to appear though not apparent. The intensity of peaks at  $1807\text{ cm}^{-1}$  and  $1773\text{ cm}^{-1}$  keep increasing with increasing EC content. More EC compound is seen to form complexes with both PCL and NH<sub>4</sub>SCN.

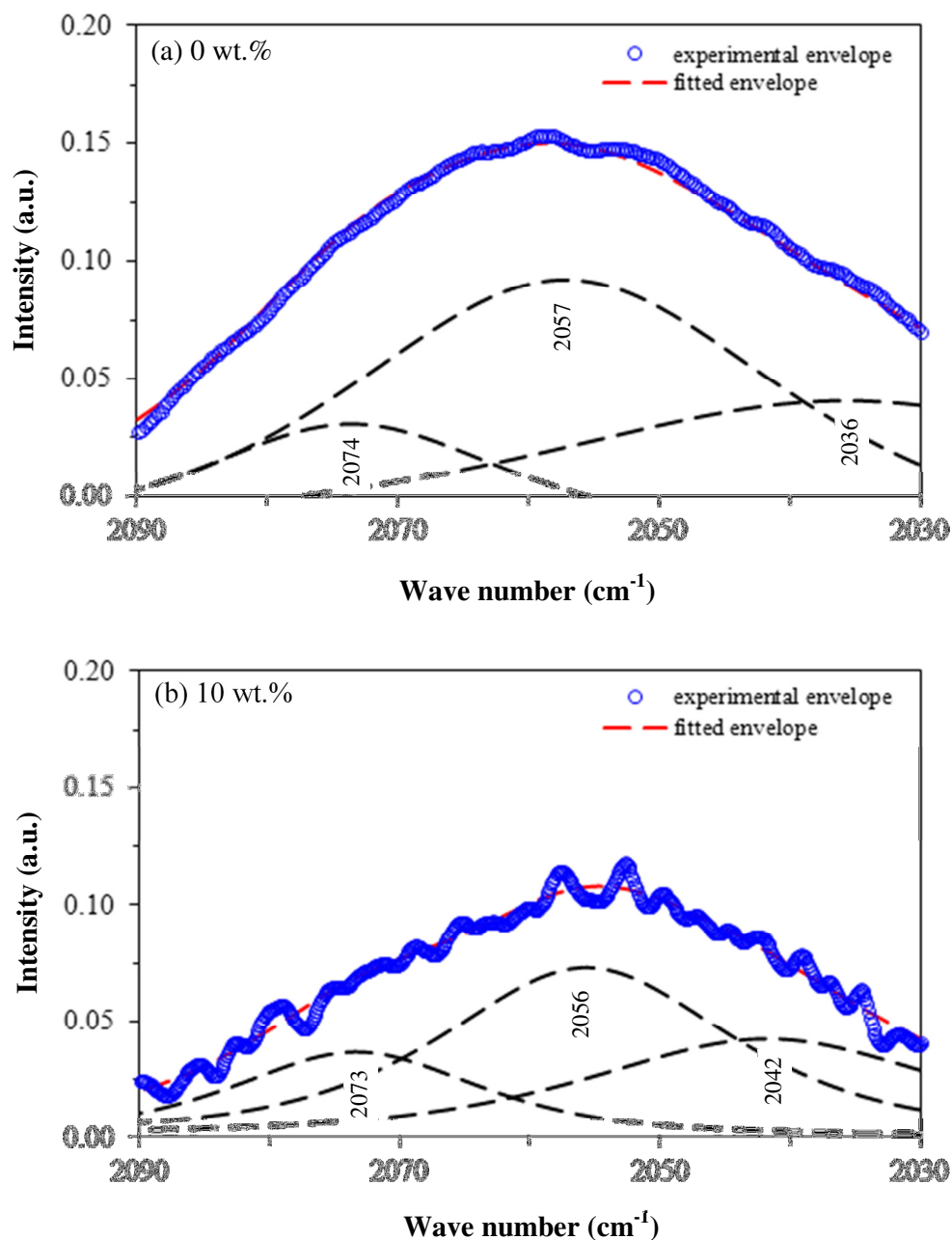
Upon addition of 40 and 50 wt.% EC concentration, the intensity of PCL carbonyl stretching at  $1720\text{ cm}^{-1}$  is reduced unexpectedly. However, the doublet peaks at  $1614\text{ cm}^{-1}$  and  $1650\text{ cm}^{-1}$  become apparent. This is most probably due to the formation of PCL-NH<sub>4</sub><sup>+</sup> complex. High EC concentration seems to encourage interaction between PCL and NH<sub>4</sub>SCN. Both peaks at  $1807\text{ cm}^{-1}$  and  $1773\text{ cm}^{-1}$  continue to increase in intensity. This indicates a stronger interaction between EC and PCL and also between EC and NH<sub>4</sub>SCN, respectively.

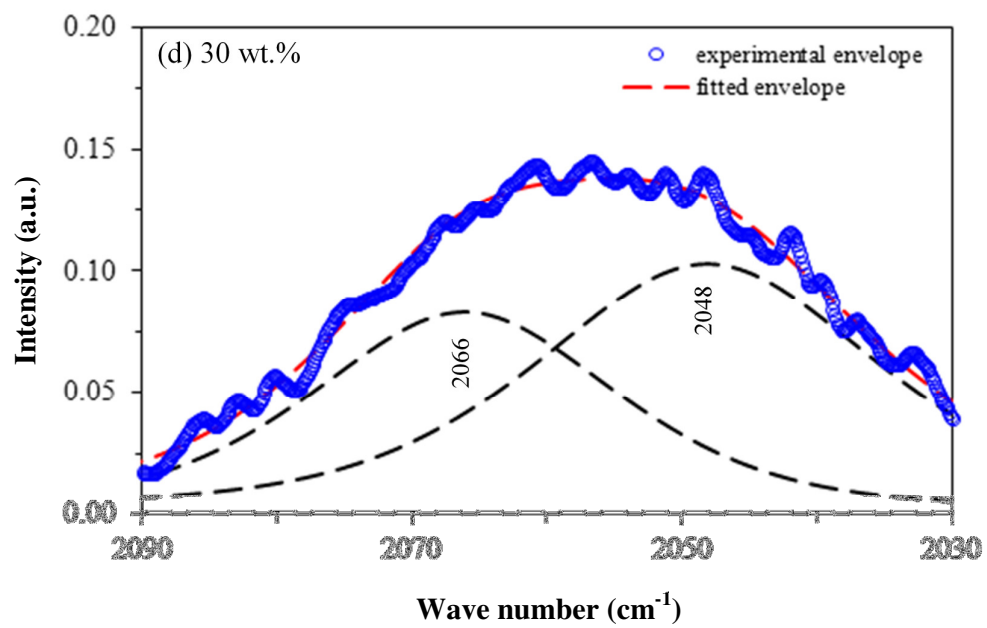
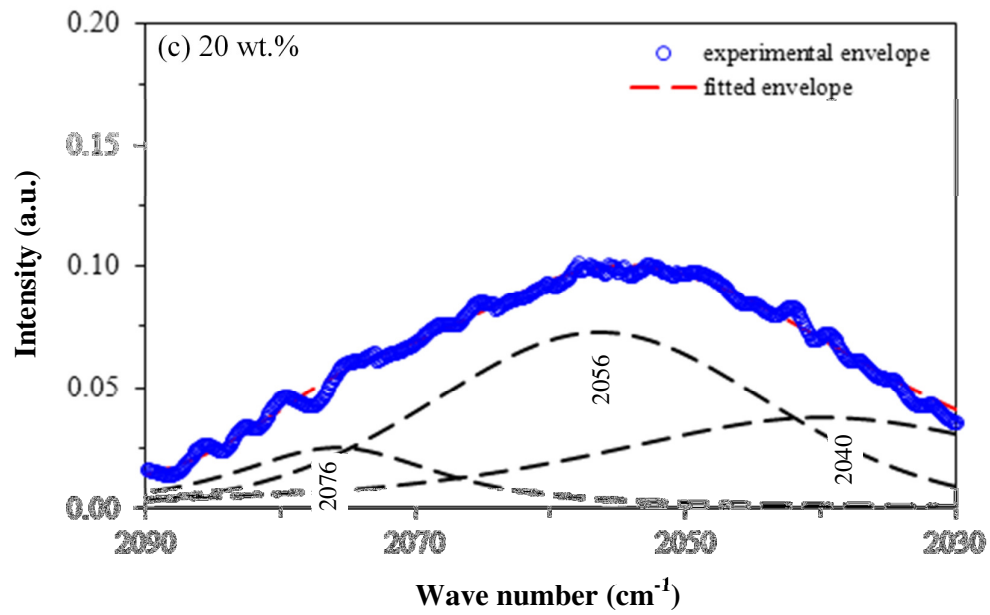
From the examination of IR spectra in the region between  $1500$  and  $1900\text{ cm}^{-1}$ , the alteration of peak intensity, appearance of new doublet peaks and frequency shifts suggest that EC is interacting with both PCL and  $\text{NH}_4\text{SCN}$  and complexation has taken place in PCL- $\text{NH}_4\text{SCN}$ -EC system. As such, the cation of the salt could interact with the carbonyl group of both PCL and EC via coordinate bond as proposed in Fig. 6.20. The addition of EC has introduced new coordinating sites or pathways for the cation to jump from one complex site to another upon an applied electric field. The effective jump distance gets shorten as depicted in Fig. 6.20. Therefore, it is expected that the activation energy for this PCL- $\text{NH}_4\text{SCN}$ -EC system is lower than the previous PCL- $\text{NH}_4\text{SCN}$  system.



**Fig. 6.20.** Schematic representation of the cation coordination in PCL- $\text{NH}_4\text{SCN}$ -EC polymer complex. The dotted line represents the ion-dipole interaction between cation and PCL and stripe line represents the dipole-dipole interaction between PCL and EC. Arrow shows the direction of the cation movement.

The transmittance spectra in the  $\text{SCN}^-$  stretching mode between 2030 and 2090  $\text{cm}^{-1}$  region are deconvoluted to study the effect of EC in ion dissociation as presented in Fig. 6.21. The integral area percentage of the ionic species is calculated and the results of individual fitted curve are displayed in Fig. 6.22 as a function of EC concentration.





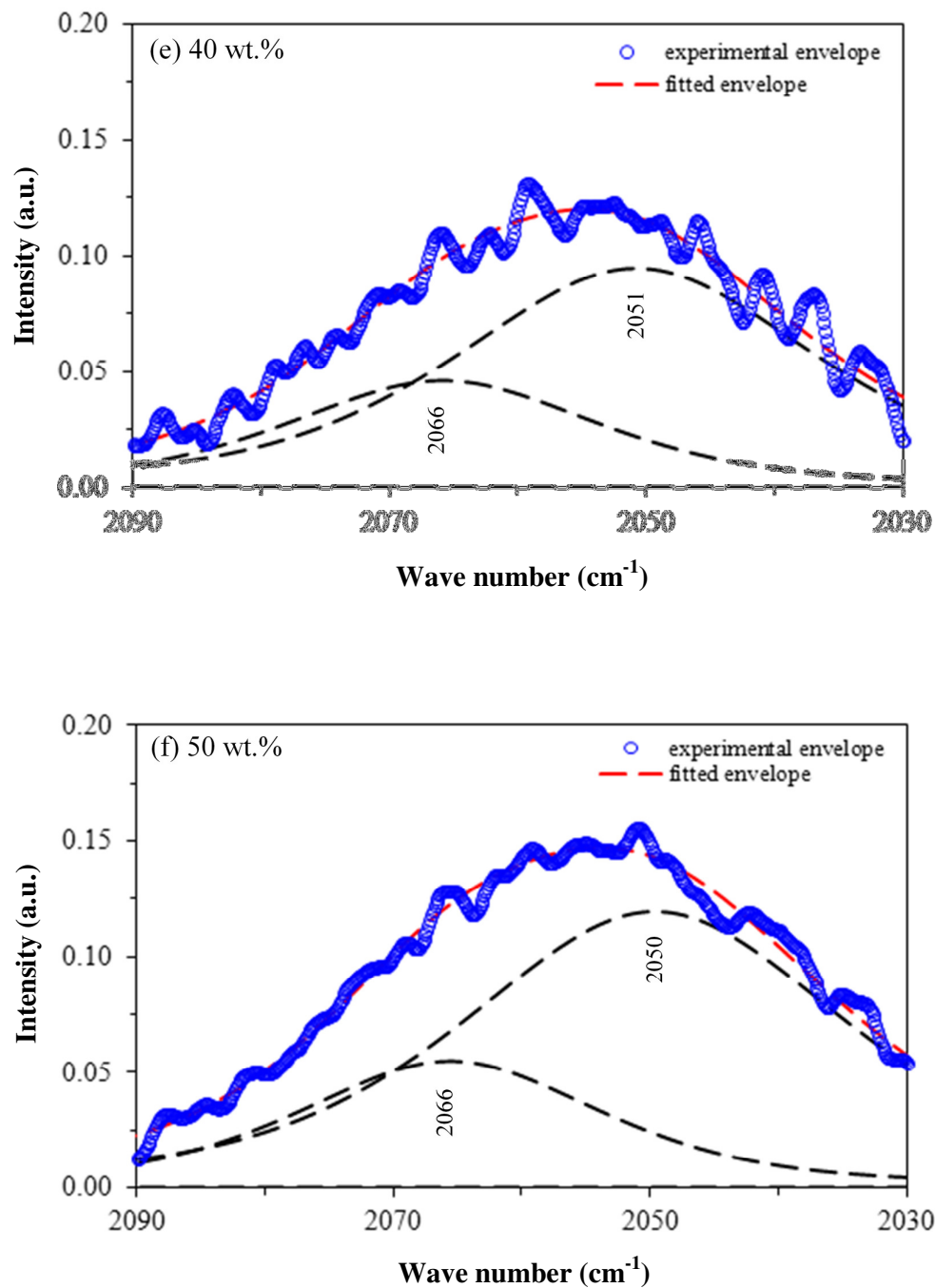


**Fig. 6.21.** The curve-fitting IR spectra of PCL-NH<sub>4</sub>SCN-EC films added with 0 to 50 wt.% EC displaying CN stretching modes.

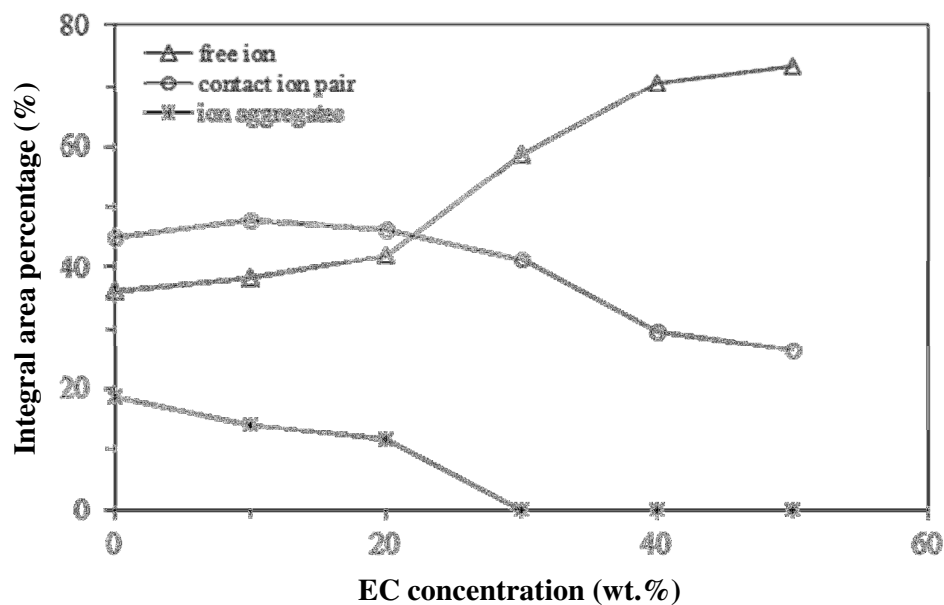


**Fig. 6.22.** Integral area percentage of free ions, contact ion pairs and ion aggregates as a function of EC concentration for PCL-NH<sub>4</sub>SCN-EC system.

When low EC concentrations (10 and 20 wt.%) are added, a steady increase of the integral area of free ions is observed from 36.0 to 38.2 and 41.9 %, respectively. At the same time, the ion aggregates decrease proportionally from 18.7 to 14.0 and 11.7 %, respectively. The number density of free ions seems to grow at the expense of ion aggregates. On the other hand, the fraction of contact ion pair at 10 wt.% EC rises slightly from 45.3 to 47.8 % but at 20 wt.% drops back marginally to 46.4 %.

Upon further incorporation of EC to 30 wt.%, the integral area percentage of free ions enhance dramatically to 58.7 %. It is therefore not surprising to observe a drastic drop of ion aggregates percentage to 0 %. This means that the entire bigger size ion aggregates are not found in the sample. Also, a considerable decrease of integral area percentage of contact ion pairs to 41.3 % is observed.

At high EC concentrations (40 and 50 wt.%), the number of free ions continue to increase consistently to 70.4 % and 73.5 %, respectively. In the absence of ion aggregates, the contact ion pairs are expected to drop accordingly to 29.6 % and 26.5 %, respectively. These results are in agreement with literature reported elsewhere [Forsyth *et al.*, 1995; Chintapalli and Frech, 1996; Kumar and Sekhon, 2002]. In PEO-LiCF<sub>3</sub>SO<sub>3</sub>-EC system of Chintapalli and Frech, their FTIR results showed that addition of EC increases the number of free ions drastically.

Kumar and Sekhon (2002) found the same conclusion in PEO-NH<sub>4</sub>F-DMA system, Forsyth and co-workers (1995) used NMR spectroscopy in PEG-NaCF<sub>3</sub>SO<sub>3</sub>-PC system to conclude that PC significantly increased the number of free sodium ions. Therefore, these deconvolution results clearly suggest that the addition of EC into PCL-NH<sub>4</sub>SCN system helps to dissociate ion pairs and higher aggregates, leading to a higher number of free ions. These results should give an insight on the conductivity studies in chapter 7.

## 6.8 Summary

For PCL-NH<sub>4</sub>SCN system:

- Upon addition of 5 wt.% salt, the carbonyl bands are observed to maintain at 1736 and 1720 cm<sup>-1</sup> but a new small peak appears at 1623 cm<sup>-1</sup>. This new peak increases in intensity as more salt is incorporated. This implies that complexation occurs between PCL and NH<sub>4</sub>SCN. NH<sub>4</sub><sup>+</sup> interacts with the

carbonyl bands of PCL in the way one of the H atom of the  $\text{NH}_4^+$  serves as coordinate bond donor while O atom of the C=O serves as coordinate bond acceptor. This conclusion also verifies DSC results obtained in section 4.2 (Fig.4.2). No traces of solvent THF is found in the complex.

- $\text{SCN}^-$  stretching mode is deconvoluted to study the ion dissociation effect. The integral area percentage of free ions increases with increasing salt content up to 26 wt.% salt. Beyond 26 wt.%, the free ions are too close to one another, forming ion pairs and higher aggregates through the coulombic force attraction. Thus, the number of free ion drops while both number of contact ion pair and ion aggregate rise. This result could give an insight in conductivity studies in chapter 7.

For PCL-EC system:

- An interaction between the PCL and EC is suggested when a new peak at  $1812\text{ cm}^{-1}$  emerges upon addition of EC. This new peak is attributed to the upshift of C=O stretching of EC from  $1784\text{ cm}^{-1}$ . The intensity of this peak increases with increasing EC content.

For EC- $\text{NH}_4\text{SCN}$  system:

- Peak shifts, peak intensity changes and merging of peaks prove EC- $\text{NH}_4\text{SCN}$  interaction. Both C=O stretching of EC at  $1784\text{ cm}^{-1}$  and  $1766\text{ cm}^{-1}$  are shifted and increase in intensity upon addition of  $\text{NH}_4\text{SCN}$ .

- Two CH<sub>2</sub> modes of EC have merged. The ring stretching, ring breathing and skeletal stretching modes display an upshift to higher wavenumber.

For PCL-NH<sub>4</sub>SCN-EC system:

- Comparative IR spectral studies at varying EC content shows that complexation are formed between EC and PCL, EC and NH<sub>4</sub>SCN. The appearance of two new peaks at 1773 cm<sup>-1</sup> and 1807 cm<sup>-1</sup> and various wavenumber shifts supports such complexation. This conclusion is also supported by DSC studies earlier in section 4.3 (Fig.4.6).
- The cation of the salt could interact with the carbonyl group of both PCL and EC. Incorporation of EC has introduced new pathways with shorter jump distance for the cation to move from one complex site to another. Therefore, it is expected that the activation energy for this PCL-NH<sub>4</sub>SCN-EC system is lower than the previous PCL-NH<sub>4</sub>SCN system.
- EC seems to be a stronger competitor than PCL for interaction with NH<sub>4</sub><sup>+</sup> of the ammonium salt.
- From the deconvolution study of SCN<sup>-</sup> stretching mode, the plot of integral area percentage helps to gain further insight on the variation of free ions. The number density of free ions seems to grow at the expense of ion aggregates. Following this, the addition of EC into PCL-NH<sub>4</sub>SCN system helps to dissociate ion pairs and higher aggregates leading to a higher number of free ions. Therefore, conductivity variation is expected to follow the variation of free ion percentage.

How does this analysis contribute to interpret conductivity studies? It will be dealt with in the following chapter.